PIP4Kβ interacts with and modulates nuclear localisation of the high activity PtdIns5P-4-kinase isoform, PIP4Kα

Yvette Bultsma, Willem Jan Keune, Nullin Divecha

PIP4Kβ interacts with and modulates nuclear localisation of the high activity PtdIns5*P*-4-kinase isoform, PIP4Kα

Yvette Bultsma, Willem-Jan Keune and Nullin Divecha*

CRUK Inositide Laboratory, the Paterson Institute for Cancer Research, Wilmslow Road, Manchester, M20 4BX, England.
Previous address: The Netherlands Cancer Institute, Plesmanlaan 121, Amsterdam. 1066CX, The Netherlands.

* To whom correspondence should be addressed: ndivecha@picr.man.ac.uk

Key words: phosphoinositide/PtdIns(4,5)P_2/PtdIns5*P*/phosphatidylinositol-5-phosphate kinase.

Running title: interaction of the alpha and beta isoforms of PtdIns5*P*-4-kinases

Subject category: signal transduction.

Abstract.

The β-isoform of phosphatidylinositol-5-phosphate (PtdIns5*P*)-4-kinase (PIP4K) regulates the levels of nuclear PtdIns5*P*, which in turn modulates the acetylation of the tumour suppressor p53. The crystal structure of PIP4Kβ demonstrated that it can form a homodimer with the two subunits arranged in opposite orientations. Using mass spectrometry, isoform specific antibodies to PIP4Ks, RNAi suppression and overexpression studies, we show that PIP4Kβ interacts *in vitro* and *in vivo* with the PIP4Kα isoform. As the two isoforms phosphorylate the same substrate to generate the same product, the interaction could be considered to be functionally redundant. However, contrary to expectation, we find that PIP4Kβ has 2000 times less activity towards PtdIns5*P*, compared to PIP4Kα and that the majority of PIP4K activity associated with PIP4Kβ comes from its interaction with PIP4Kα. Furthermore, PIP4Kβ can modulate the nuclear localisation of PIP4Kα and PIP4Kα has a role in regulating PIP4Kβ functions. Our data present a rational for the functional interaction between PIP4Kα and PIP4Kβ and provide insight into how the relative levels of the two enzymes may be important in their physiological and pathological roles.

Introduction.

Combinations of phosphorylation at the 3,4, or 5, position of the inositol head group of phosphatidylinositol generates seven different phosphoinositides that form the basis of a ubiquitous membrane signalling system. An array of tightly regulated phosphoinositide kinases and phosphatases, ultimately control the subcellular profile of phosphoinositides [1]. Phosphoinositides can regulate protein localisation, ion channel function and protein enzymatic activity, which can impact on cellular processes including vesicle transport, cytoskeletal dynamics, cell proliferation and survival, gene transcription, cell polarity and migration [2].

Phosphatidylinositol(4,5)bisphosphate (PtdIns(4,5)P_2) is central to phosphoinositide signalling being a substrate for both phospholipase C (PLC) and phosphatidylinositol-3-kinase (PtdIns-3-kinase) and itself a second messenger [3]. PtdIns(4,5)P_2 can be synthesised by two different enzyme families that are highly related. Phosphatidylinositol-4-phosphate (PtdIns4*P*)-5-kinases (PIP5Ks) phosphorylate PtdIns4*P* [4] on the 5-position while phosphatidylinositol-5-phosphate (PtdIns5*P*)-4-kinases (PIP4Ks) phosphorylate PtdIns5*P* on the 4-position [5]. The cellular level of PtdIns4*P* is much greater than PtdIns5*P* and it is likely that the majority of PtdIns(4,5)P_2, in the cell, is synthesised through PIP5K activity. In accord with this hypothesis, overexpression or suppression of different isoforms of PIP5K impinge on many of the processes known to be regulated by PtdIns(4,5)P_2 [3]. In contrast to PIP5Ks, the role of PIP4Ks is less well understood. Of the three isoforms of PIP4K [6-9], the α and β isoforms can phosphorylate PtdIns5*P* and PtdIns3*P* [10], while the γ isoform is likely to be inactive. PIP4Kγ, however, can interact with PIP4Kα and β, probably to target their activities to a particular subcellular localisation [11].

Overexpression of PIP4Ks does not lead to phenotypes that are induced by PIP5Ks, suggesting that PIP4Ks do not increase the cellular level of PtdIns(4,5)P_2 to the same extent as PIP5Ks. However, this may only reflect the relative levels of PtdIns5*P* to PtdIns4*P* in the cell. In megakaryoctyes, for example, PIP4Kα-mediated synthesis of PtdIns(4,5)P_2 is important in platelet formation [12] and in platelets it is required for secretion [13;14]. Deletion of the only PIP4K in *C.elegans* and *D.melanogaster* led to an increase in whole animal levels of PtdIns5*P* (our unpublished data) and in murine erythroleukemia cells (MEL), RNAi-mediated suppression of PIP4Kβ increased, while the overexpression of PIP4Kβ decreased the levels of nuclear PtdIns5*P* [15]. These data suggest that PIP4Ks, through phosphorylation, likely control the level of PtdIns5*P*.

The relative expression level of PIP4K isoforms varies in mouse tissues. For example, in brain, PIP4Kα and β are approximately equal while there is nearly 10 fold more PIP4Kβ mRNA in muscle and in the heart. In the spleen, PIP4Kα expression is 3-4 fold higher than PIP4Kβ. PIP4Kγ, on the other hand, is highly expressed in the kidney [11]. The differential expression suggests that each PIP4K may have specific functions within the target organ. At a cellular level, PIP4Kα localises in the cytosol, while PIP4Kγ associates with an endomembrane compartment that partially co-localises with the golgi [9;11]. PIP4Kβ appears to localise predominantly in the nucleus [16]. However, PIP4Kβ interacts with both a TNF receptor [8] and the EGF receptor [17] suggesting that it may also be required in the cytosol. Deletion of

PIP4Kβ in mice leads to increased insulin-induced PKB activation in muscle [18] and in cells, overexpression of kinase active but not kinase inactive PIP4Kβ attenuates insulin induced PKB activation [19]. Finally, overexpression of IpgD, a bacterial PtdIns(4,5)P_2-4-phosphatase that generates PtdIns5*P*, also increased PKB activity [19]. Together, these data point to a role for cytosolic PIP4Kβ and PtdIns5*P* in PKB activation, possibly through the regulation of PtdIns(3,4,5)P_3 [19] and/or PKB dephosphorylation [20].

PIP4Kβ is also present in the nucleus and its nuclear import is dictated by a sixteen amino acid α-helical insertion [16] that is not present in other PIP4Ks. In the nucleus, activation of the p38 stress pathway inhibits PIP4Kβ activity leading to an increase in PtdIns5*P*. PtdIns5*P* can interact with the PHD finger of inhibitor of growth protein 2 (ING2) [21], which in turn modulates the acetylation and transcriptional activity of the tumour suppressor protein p53 [15]. PHD finger containing proteins appear to be nuclear specific downstream targets of PtdIns5*P* [22;23]. Through its interaction with SPOP (speckle-type POZ protein), PIP4Kβ can regulate the activity of the CUL3 (Cullin 3) ubiquitination complex. The CUL3 ubiquitination activity also appears to be stimulated by increased levels of PtdIns5*P* [24].

The differential tissue expression and sub-cellular localisation of PIP4Ks provides a reasonable explanation for the requirement for different isoforms within a cell. However, during a search for proteins that regulate PIP4Kβ, we discovered that PIP4Kβ interacts with PIP4Kα. Previous studies indicate that PIP4Kα and PIP4Kβ phosphorylate the same substrate to generate the same product suggesting that their interaction may have no functional advantage. Here we have studied the activity of both enzymes *in vitro* and *in vivo* and together with RNAi and overexpression assays have developed a rational for a functional interaction between PIP4Kα and PIP4Kβ.

Materials and methods.

PIP4K plasmids, Antibodies and chemicals.

GST-PIP4Kα and β, EE-PIP4Kα, EE-PIP4KαKD (G131L/Y138F), Myr-PIP4Kα and HA-PIP4Kβ were derived from human sequences. Myc-PIP4Kα and Myc-PIP4Kβ and Myc-PIP4KβKD (D278A) were derived from rat sequences. Peptides (p5:CGVGGNLLCSYG, p6: CNLLSFPRFFGP, p19: CMATPGNLGSSVL) were coupled to keyhole limpit hemocyanin and used to immunise New Zealand white rabbits (for specificity of the antibodies see supplementary figure 2). Antibody 3 is a rat monoclonal that was previously described [25]. The anti-PIP4Kα-C-term was from Abgent (AP8041b). Anti-HA and anti-Myc are monoclonal supernatants from clone 12CA5 and 9E10 respectively. Protein G and A sepharose, glutathione sepharose and Ni sepharose were purchased from GE Healthcare. Disuccinimidyl suberate (DSS) was from Pierce chemicals. All other chemicals were of analar grade.

Generation of HEK293 cells stably expressing shRNAi.

ShRNAi constructs, generated by cloning the following sequences into pRetroSuper, were used to generate viral particles in Phoenix ecotropic cells.
RNAi-PIP4Kα: 5'-ATAGTGGAATGTCATGGGA-3',
RNAi-PIP4Kβ: 5'-AGATCAAGGTGGACAATCA-3'
.
HEK293 cells, stably expressing the ecotropic receptor, were infected with retroviral particles using polybrene. Cell populations were selected using puromycin (2μg/ml). In general, cells were maintained in the absence of the antibiotic selection for at least 48 hours prior to the experiments.

SiRNA targeting of PIP4Ks.

Control SiRNA oligos (siGENOME Non-Targeting siRNA Pool, Dharmacon, D-001206-13-20) or those targeting PIP4Kα (PIP4K2A siGENOME SMARTpool, Dharmacon) M-006778-01) or PIP4Kβ (PIP4K2B siGENOME siRNA D-006779-02, D-006779-04, D-006779-06) were transfected into HEK293 cells using Dharmafect 1. Forty eight hours later cell lysates were used in immunoprecipitation experiments.

PIP4K activity measurements and PtdIns5*P* mass measurements.

In vitro PIP4K activity was measured using liposomes with 1 nmol PtdIns5P and 10 nmol of phosphatidylserine (PtdSer) as a substrate, 20 μM ATP, 10 μCI ^{32}P-ATP and the appropriate amount of enzyme in 100 μl of PIPKIN buffer (50 mM Tris-HCl pH 7.4, 10 mM $MgCl_2$, 1 mM EGTA, 70 mM KCl) for 10 minutes. The reactions were terminated and extracted as previously described [26]. ^{32}P-PtdIns(4,5)P_2, a measure of PIP4K activity, was separated by TLC and quantitated using a phosphoimager (Biorad). To determine how PIP4K activity varied with respect to the levels of PtdIns5*P*, liposomes were made with 50nmol of PtdSer and varying amounts of PtdIns5*P*. Phosphoimager counts were converted to μmol of PtdIns(4,5)P_2 by quantitating standard amounts of ^{32}P-ATP spotted on to the TLC. Vmax was determined at a saturating concentration of PtdIns5*P* and the Km was determined graphically at 50% of the Vmax value. PtdIns5*P* was measured as described [26].

Subcellular fractionation and cross-linking

MEL cell nuclei were purified as previously described [27] except that the final resuspension buffer (FRB, see below) was made with 10 mM HEPES instead of Tris

to prevent quenching of the cross-linker. Nuclei, controls or treated with the indicated concentrations of cross-linking agent (Disuccinimidyl suberate DSS) were terminated by the addition of 1 M glycine pH7.5 (20 mM). Nuclear proteins were extracted using FRB (see below) containing 1% CHAPS, 0.5 M NaCl and immunoprecipitated using the indicated antibody. Immune-complexes were collected on proteinG sepharose and were solubilised using 1x SDS-PAGE loading buffer, separated by SDS-PAGE and analysed by western blotting.
HEK293 cells were trypsinised, washed with PBS and resuspended in hypotonic swell buffer (5 mM Tris-HCl pH 7.4, 1.5 mM KCl, 2.5 mM $MgCl_2$) for six minutes on ice. The cells were then disrupted by passage through a 22 gauge needle. The nuclei were pelleted by centrifugation (4 minutes, 352xg, 4^{o}C) and the supernatant was removed and membranes were collected by high speed centrifugation (14000rpm microfuge) at 4^{o}C for 15 minutes. The supernatant (cytosol) was collected and the membranes were sonicated into FRB (membrane fraction). The nuclei were further purified by centrifugation through a sucrose cushion (10 mM Tris-HCl pH 7.4, 1 mM EGTA, 1.5 mM KCl, 5 mM $MgCl_2$, 460 mM sucrose) and washed with final resuspension buffer (FRB 10 mM Tris-HCl pH 7.4, 1 mM EGTA, 1.5mM KCl, 5 mM $MgCl_2$, 290 mM sucrose). Nuclei were resuspended in FRB or were extracted by resuspending them in Dignam C buffer (20 mM Tris pH7.9, 0.42 M NaCl, 1.5 mM MgCl2, 0.2 mM EDTA, 25% glycerol, 0.5 mM DTT) followed by incubation on ice for 30 minutes. The insoluble fraction was pelleted by centrifugation and the supernatant was dialysed against Dignam D buffer (20 mM Tris pH7.9, 0.1 M KCl, 0.2 mM EDTA, 10% glycerol, 0.5 mM DTT) and samples were stored at -80°C.

Sucrose density centrifugation.
1 ml each of 40%, 31.25%, 22.5%, 13.72% and 5% sucrose solutions were layered sequentially in a centrifuge tube and allowed to form a gradient overnight by standing at 4^{o}C. The cytosol (50 µl) and nuclear fraction (50 µl) were adjusted to 5% sucrose and loaded on top of the cushions and then centrifuged for 18 hours at 45000 rpm. After centrifugation fifteen 1 ml fractions were isolated from the bottom of the centrifuge tube using a syringe and needle. The samples were mixed with SDS-loading buffer separated by SDS-PAGE and analysed by staining the gel or by western blotting.

Mass spectrometry

Gel band destaining and washing
Coomassie blue stained gel bands were destained with three twenty minute changes of 1ml 200mM ammonium bicorbante, 40% (V/V) acetonitrile. Gel bands were the dehydrated by the addition of 500ul acetonitile for fifteen minutes followed by rehydration in 500ul of water for a further fifteen minutes. This dehydration-rehydration procedure was performed a total of three times followed by a final dehydration in acetonitrile.

In-Gel tryptic digestion
Gel bands were rehydrated in 25ul of 50mM ammonium bicarbonate, 9% (v/v) acetonitrile, 20ng/ul sequencing grade trypsin (Sigma-Aldrich) for twenty minutes. The bands were then covered in 100ul of 50mM ammonium bicarbonate, 9% (v/v) acetonitrile and incubated at 37^{o}C for 18hrs. Following digestion, samples were acidified by the addition on 10ul of 10% (v/v) formic acid. The digest supernatant

was then transferred to a fresh eppendorf tube and the digest was dried in a vacuum centrifuge at 40°C for 30 minutes. The dried peptides were then resuspended in 20ul of water, 0.1% trifluoroacetic acid (Sigma-Aldrich) prior to LCMS analysis.

nLCMSMS Analysis

Peptides were separated utilising a Nano-Acquity UPLC system (Waters) as detailed below. Sample was loaded onto a Waters C18 Symmetry trap column (180um ID, 5um 5cm) in water, 0.1% (v/v) acetonitrile, 0.1% (v/v) formic acid at a flow rate of 7ul/min for 5 minutes. Peptides were then separated using a Waters NanoAcquity BEH C18 column (75um ID, 1.7um, 25cm) with a gradient of 3 to 30% (v/v) of acetonitrile, 0.1% formic acid over 30 minutes at a flow rate of 400nl/min. The nLC effluent was sprayed directly into the LTQ-Orbitrap XL mass spectrometer aided by the Proxeon nano source at a voltage offset of 2.5KV. The mass spectrometer was operated in parallel data dependent mode where the MS survey scan was performed at a nominal resolution of 60, 000 (at m/z 400) resolution in the Orbitrap analyser between m/z range of 400-2000. The top 6 multiply charged precusors were selected for CID in the LTQ at a normalised collision energy of 35%. Dynamic exlusion was enabled to prevent the selection of a formally targeted ion for a total of 20 seconds.

Immunoprecipitations.

Washed cells were resuspended in lysis buffer (50 mM Tris pH 8.0, 50 mM KCl, 10 mM EDTA, 1% NP-40,) and after 15 minutes the nuclei and cell debris were removed by centrifugation (14000 rpm, microcentrifuge 4°C, 10 mins). Lysates were incubated with the appropriate antibodies overnight and immune-complexes were captured using proteinG sepharose (1 hour 4°C). Immunoprecipitates were washed three times with IP wash buffer (50 mM Tris pH 7.5, 150 mM NaCl, 5 mM EDTA, 0.1% Tween-20), resuspended in 1xSDS-loading buffer and subjected to SDS-PAGE and transferred to nitrocellulose. After incubation with the indicated antibodies, antibody/protein interactions were detected with ECL (GE Healthcare) or super signal (Pierce chemicals).

SDS-PAGE and Western blotting

Protein extracts were quantitated using the BIORAD reagent and adjusted to 1X SDS-loading buffer. After boiling, the extracts were either treated or not with iodoacetamide to modify cysteine residues and then separated by SDS-PAGE. Proteins were transferred to nitrocellulose, blocked in PBS-T-5%fat free milk for 1 hour and then incubated with the primary antibody appropriately diluted in Magic mix (PBS-0.1% Tween 20 (PBS-T), 1% western blocking reagent (Roche), 3% BSA). Antibody dilutions used were: p19 and p6 1:10000, anti-PIP4Kα-C-term 1:1000, anti-Myc 1:100, anti-HA 1:100. The blots were washed with PBS-T and then incubated with the appropriate HRP-conjugated secondary antibody diluted in Magic mix (anti-Rabbit, mouse and rat 1:10000 (GE H), Anti-rabbit-TrueBlot (eBioscience) 1:10000). Antibody-protein interactions were visualised using ECL (GE H) or super signal (Pierce). Blots were stripped by incubation at 55°C in 50ml of strip buffer (50 mM TRIS pH 7.4, 2% SDS, 50 mM β-mercaptoethanol) for 20 minutes followed by extensive washing in PBS-T. The blots were blocked again and then used as above.

Production of recombinant proteins.

Bacterial colonies transformed with the appropriate vector were diluted into 5 ml of LB medium containing ampicillin (50 μg/ml) and grown overnight. Cultures were diluted to 100 ml, grown at 37°C for 1 hour and then IPTG (100 μM final concentration) was added and the cultures were grown overnight at 30°C. Cells were collected by centrifugation (4000 rpm for 10 minutes), washed with PBS and resuspended in 5 mls of PBS. Cells were disrupted by sonication (Diagenode cell disruptor set at the high intensity setting) and Triton-X-100 was added to a final concentration of 1%. Cell debris was removed by centrifugation and the supernatant was incubated with Glutathione sepharose beads for 2 hours. After extensive washing (PBS-1% Triton-X-100), the bound proteins were eluted using 10mM reduced glutathione in 50 mM Tris pH 8, 0.3 M NaCl. Eluted proteins were quantitated using BIORAD reagent and by SDS-PAGE and coomassie blue staining and dialysed into an appropriate buffer. GST was cleaved by incubation with thrombin for 2 hours at room temperature. The uncleaved protein and the cleaved GST-portion were removed by an additional incubation with glutathione sepharose. The cleaved protein was quantitated using standardised amounts of BSA after SDS-PAGE electrophoresis and coomassie blue staining.

HEK293 cells were transfected with the appropriate plasmid encoding a HA-tagged protein using calcium phosphate. The transfected cells were washed once with cold PBS, trypsinised and lysed in lysis buffer. The HA-tagged protein was immunopurified by using the anti-HA antibody followed by protein-G sepharose. After extensive washing with IP wash buffer, the HA-tagged protein was eluted with 3XHA peptide (YPYDVPDYA) (1 mg/ml in 50 mM Tris pH 8, 0.3 M NaCl) by incubation at 30°C for 30 minutes. The eluted protein was quantitated using standardised amounts of BSA after SDS-PAGE electrophoresis and coomassie blue staining.

Reconstitution of PIP4Kα/PIP4Kβ complexes using recombinant proteins.
Cleaved bacterially expressed PIP4Kα was incubated alone or together with HA-PIP4Kβ in a volume of 150μl of PIPKIN buffer containing 0.1% NP40, 1 μg/ml BSA, 15 mM dithiothreitol for one hour. The complexes were collected by HA-immunoprecipitation overnight at 4°C and were separated by SDS-PAGE and analysed by western blotting.

Ubiquitination assays.
HEK293 cells were transfected using calcium phosphate. MG-132 (10 μM) was added for the final 6 hours, then the cells were washed once with PBS and lysed directly into PBS-0.2% SDS, 8 M urea and sonicated. His-tagged proteins were purified on Ni columns and separated using SDS-PAGE and analysed by western blotting.

Confocal microscopy.
HeLa cells were transfected on glass coverslips using Fugene. HT1080 cells were transduced with the constructs indicated, selected with the appropriate antibiotics and plated on coverslips. The cells were fixed using PBS-4% formaldehyde (20 minutes), permeabilised with PBS-0.1% triton-X100 (5 minutes) and blocked with PBS-3% BSA (10 minutes). Appropriate antibodies were diluted in PBS-3% BSA and incubated with the coverslips for 30 minutes at 37°C in a humidified incubator. The coverslips were washed with PBS and incubated for 30 minutes with fluorophore-conjugated secondary antibodies diluted appropriately in PBS-3%BSA. The

coverslips were mounted using Vectashield, sealed using nail varnish and analysed by confocal microscopy (Zeiss)

Results.

PIP4Kβ complexes.

In order to study the localisation of PIP4Kβ and identify proteins that interact with it, a cell line expressing HA-tagged PIP4Kβ (HA-PIP4Kβ) was generated. Cytosolic and nuclear extracts were isolated from these cells and were further fractionated using sucrose gradient centrifugation. Protein molecular weights between 67 and 230 kDa could be separated (supplementary Figure 1A and B) and the BRG1 chromatin remodelling complex (MWt>500000 kDa) eluted in fractions 12-15 (Figure 1A). Cytosolic HA-PIP4Kβ eluted between a molecular weight of 120 and 200, while the nuclear HA-PIP4Kβ eluted with a molecular weight between 120 and 150 kDa (Figure 1A), however, the monomeric form of PIP4Kβ (49 kDa), which should elute in fractions 4-6, was not seen. The observed molecular weight suggested that PIP4Kβ exists only in complexes in both the cytosol and in the nucleus.

To assess if the endogenous nuclear PIP4Kβ is also in complexes, isolated nuclei from MEL cells were treated with increasing concentrations of a non-hydrolysable cross-linking agent (DSS), immunoprecipitated and analysed by SDS-PAGE and immunoblotting. Increasing concentrations of the cross-linker induced the loss of the monomeric 49 kDa protein resulting in the appearance of a 97 kDa complex. Higher concentrations of DSS resulted in disappearance of the dimeric complex possibly through irreversible cross-linking of PIP4Kβ into the nuclear pellet or cross-linking dependent loss of the epitope recognised by the antibodies (Figure 1B). The data suggest that endogenous nuclear PIP4Kβ is predominantly a dimer, which is in line with previous data obtained from the crystal structure of the PIP4Kβ [28], although higher molecular weight complexes were also seen (Figure 1C). Extraction of nuclear proteins with CHAPS/NaCl or with RIPA buffer, before the addition of the cross-linking agent, did not prevent the formation of the 97 kDa PIP4Kβ dimer, demonstrating the strength and stability of the complex (Figure 1C).

PIP4Kβ associates with PIP4Kα.

To identify potential interacting partners of PIP4Kβ, an immunoprecipitate of HA-PIP4Kβ was separated by SDS-PAGE and stained with coomassie blue. The gel was cut into 60 slices, all of which were analysed by mass spectrometry (Figure 2A). In slices 33 and 34, corresponding to a molecular weight of approximately 49 kDa, 14 peptides were identified, three of which uniquely identified PIP4Kβ and two identified PIP4Kα (Figure 2A). The data suggested that endogenous PIP4Kα interacts with HA-PIP4Kβ. To further investigate the interaction between PIP4Kα and PIP4Kβ, lysates from HEK293 cells overexpressing Myc-PIP4Kβ were used for affinity purification using bacterially expressed and purified GST, GST-PIP4Kα, GST-PIP4Kβ or GST-PIP4Kγ (Figure 2B). GST-PIP4Kα, β and γ could affinity purify Myc-PIP4Kβ but GST alone could not. To demonstrate that the interaction between PIP4Kα and PIP4Kβ occurs *in vivo*, lysates from HEK293 cells, expressing EE-PIP4Kα either alone or with HA-PIP4Kβ, were immunoprecipitated with the anti-EE or HA antibody and analysed by western blotting. Immunoprecipitation with the

anti-HA antibody affinity captured EE-PIP4Kα only when both proteins were co-overexpressed. When the reciprocal experiment was carried out, HA-PIP4Kβ was co-immunoprecipitated by the anti-EE only when both proteins were also co-expressed (Figure 2C).

To demonstrate that the interaction between PIP4Kα and β is direct, both proteins were purified, combined *in vitro* and were analysed by HA-immunoprecipitation followed by western blotting (Figure 2D). The blot also shows 10% of the PIP4Kα and β input. The anti-HA antibody immunoprecipitated approximately 80% of HA-PIP4Kβ and when HA-PIP4Kβ was combined with PIP4Kα, the anti-HA antibody immuno-affinity purified approximately 80-90% of the PIPKα showing that PIP4Kα and PIP4Kβ can interact directly (Figure 2D).

To demonstrate that endogenous PIP4Kα and PIP4Kβ can interact *in vivo* we developed two antibodies, p5 and p6, which are specific for PIP4Kβ and one antibody, p19, which is specific for PIP4Kα (supplementary data Figure 2). As the molecular weights of PIP4Kα and PIP4Kβ are identical, HEK293 cell lines, in which PIP4Kα or PIP4Kβ expression was stably suppressed by RNAi, were used for co-immunoprecipitation studies to further ensure specificity. The ShRNAi construct targeting PIP4Kα decreased PIP4Kα protein levels to 54%, while targeting PIP4Kβ decreased PIP4Kβ protein levels to 15% (Figure 3A). Pre-immune antibodies did not immunoprecipitate either PIP4Kα or β. Both p5 and p6 immunoprecipitated endogenous PIP4Kβ and co-immunoprecipitated endogenous PIP4Kα. The specificity was demonstrated by the lack of co-immunoprecipitation of PIP4Kα when its expression was suppressed using RNAi (Figure 3B). Immunoprecipitation of endogenous PIP4Kα also co-immunoprecipitated endogenous PIP4Kβ and the interaction was specific as RNAi mediated suppression of PIP4Kα reduced the co-immunoprecipitation of PIP4Kβ (Figure 3C). The data show that PIP4Kα and PIP4Kβ interact directly and that the interaction occurs *in vivo* between endogenous PIP4Kα and PIP4Kβ.

PIP4Kβ has 2000 times less PIP4K activity compared to PIP4Kα.

PIP4Kα and β phosphorylate the same substrate to generate the same product and so it is questionable why they would interact with each other. The interaction may be fortuitous, as the two proteins are highly related or alternatively, the interaction may modulate each others activities and/or their localisation. In order to rationalise why PIP4Kα and PIP4Kβ interact with each other, their enzymatic activity towards PtdIns5*P* was reassessed. GST-PIP4Kα and β were expressed in bacteria, purified and quantitated by SDS-PAGE and coomassie blue staining (Figure 4A). Both enzymes phosphorylated PtdIns5*P* on the 4-position, to generate PtdIns(4,5)P_2, as demonstrated by dephosphorylation of the product with a specific recombinant PtdIns(4,5)P_2-5-phosphatase (data not shown). Therefore, both PIP4Kα and β are *bona fide* PtdIns5*P*-4-kinases. However, PIP4Kα phosphorylated PtdIns5*P* approximately 434 fold better than PIP4Kβ (Figure 4A). As the difference in activity between the PIP4Kα and β could be a consequence of their expression in bacteria, Myc-tagged proteins, expressed in and purified from HEK293 cells, were tested for PIP4K activity. As observed with the bacterially expressed proteins, PIP4Kα had approximately 207 times more activity than PIP4Kβ (Figure 4B). To determine more

accurately the difference in PIP4K activity between PIP4Kα and β, we assessed the activity of bacterially expressed PIP4Kα and β at different concentrations of PtdIns5*P* presented in phosphatidylserine liposomes (Figure 4C). The data show that while both enzymes had approximately the same Km with respect to PtdIns5*P*, the Vmax of PIP5Kα was 2000 fold higher than PIP4Kβ (see table for quantitation). To assess whether PIP4Kα and PIP4Kβ have the same activity *in vivo*, cellular PtdIns5*P* levels were measured after the co-expression of each PIP4K isoform with a PtdIns(4,5)P_2 4-phosphatase (IpgD), which increases the level of PtdIns5*P* *in vivo* [29]. The co-expression of PIP4Kα partially attenuated an increase in the level of cellular PtdIns5*P* induced by the expression of GFP-IpgD. In contrast, expression of an equivalent amount of PIP4Kβ did not attenuate the IpgD induced increase in PtdIns5*P* (Figure 4D). This was not a consequence of the nuclear localisation of PIP4Kβ as we show, here (Figure 6C) that overexpressed PIP4Kβ is localised in the cytoplasm, nucleus and at the plasma membrane in HeLa cells. These data show that *in vitro* and *in vivo*, PIP4Kβ is much less active compared to PIP4Kα.

PIP4Kα provides the majority of PIP4K activity in PIP4Kβ immunoprecipitations. To determine if PIP4Kα provides the majority of PIP4K activity in a heteromeric complex, PIP4K activity was assessed in complexes containing either wild type or kinase inactive EE-PIP4Kα. Overexpression of EE-PIP4Kα led to a dramatic increase in PIP4K activity in the EE-immunoprecipitate that, as expected, was not present when an inactive EE-PIP4Kα kinase was expressed (Figure 5A). Co-overexpression of wild-type HA-PIP4Kβ did not lead to any changes in PIP4K activity associated with the EE-immunoprecipitation but as expected HA-PIP4Kβ was co-immunoprecipitated as assessed by western blotting (Figure 5A). Overexpression of HA-PIP4Kβ induced a very small increase in PIP4K activity associated with the HA-immunoprecipitate, however, when EE-PIP4Kα was co-expressed with HA-PIP4Kβ there was a 20 fold increase in PIP4K activity associated with the HA-PIP4Kβ immunoprecipitate (Figure 5A). Co-overexpression of the kinase inactive PIP4Kα actually decreased the amount of PIP4K activity associated with the HA-immunoprecipitate. The level of HA-PIP4Kβ in the various immunoprecipitates was similar (21163, 16891 and 15280 arbitrary imager units) suggesting that the changes in PIP4K activity were a consequence of co-immunoprecipitation of active EE-PIP4Kα.

To determine to what extent of the PIP4K activity associated with PIP4Kβ is due to its interaction with PIP4Kα, we stably suppressed the expression of PIP4Kα and assessed the PIP4K activity in an immunoprecipitation of endogenous PIP4Kβ. RNAi-targeting of PIP4K decreased the level of PIP4Kα protein by approximately 50% (Figure 3A) and PIP4K activity was also decreased by about 50-70% in isolated membrane, cytosol and nuclear fractions (Figure 5B). When endogenous PIP4Kβ was immunoprecipitated from the cytosol/membrane or nuclear fractions of cells suppressed for the expression of PIP4Kα, the associated PIP4K activity decreased by about 50% (Figure 5C), although the amount of PIP4Kβ immunoprecipitated remained similar (6601, 9288, 7838 and 7227 (arbitrary image units) respectively in the four separate immunoprecipitations). We also carried out a similar analysis using cells transiently transfected with siRNA oligos targeting either PIP4Kα or β. Suppression of PIP4Kα decreased PIP4Kα protein (6314 to 487 arbitrary imager

units) assessed by western blotting, while PIP4K activity in a PIP4Kα immunoprecipitate decreased to 27% of the control (Figure 5D). Similarly, suppression of PIP4Kα decreased the PIP4K activity in a PIP4Kβ immunoprecipitate to 34% of control. Suppression of PIP4Kβ as expected diminished the PIP4K protein levels (33205 in the control to 5554 (arbitrary imager units) in the siRNA PIP4Kβ) and the PIP4K activity in the PIP4Kβ immunoprecipitate to 28% of the control (Figure 5D). These data are consistent with the PIP4Kα subunit providing the majority of PIP4K acitivity present in a PIP4Kβ immunoprecipitate.

To investigate if active PIP4Kβ is required in the complex, we measured the PIP4K activity of either active or inactive Myc-PIP4Kβ in complex with the endogenous PIP4Kα. Suppression of the expression of PIP4Kα reduced the PIP4K activity associated with the immunoprecipitate of Myc-PIP4Kβ by 75% showing that the majority of activity comes from the endogenous PIP4Kα subunit (Figure 5E). Strikingly, the PIP4K activity associated with kinase inactive Myc-PIP4Kβ was also reduced to 24% compared to that associated with the active Myc-PIP4Kβ (Figure 5E). Immunoblotting showed that wild type and kinase inactive Myc-PIP4Kβ co-immunoprecipitated the same amount of endogenous PIP4Kα (3363 in the wild type PIP4Kβ immunoprecipitate compared with 3574 (arbitrary units) in the kinase inactive PIP4Kβ immunoprecipitate). The specificity of the co-immunoprecipition of endogenous PIP4Kα was demonstrated by the decrease in the PIP4Kα band in the knockdown (505 and 400 arbitrary units). Both the wild type and the kinase inactive PIP4kβ were immunoprecipitated to similar extents (21878 and 24723 in the pRetro-super cells compared with 20903 and 23537 (arbitrary imager units) in the RNAiPIP4Kα cells). These data suggest that PIP4Kα can either activate PIP4Kβ in the complex or that the kinase activity of PIP4Kβ is required for optimal PIP4Kα activity.

PIP4Kβ can modulate the localisation of PIP4Kα.

To determine whether PIP4Kβ can modulate the total amount of nuclear PIP4Kα, the level of endogenous PIP4Kα was determined in cytosol and nuclear fractions from HEK293 cells stably suppressed for PIP4Kβ expression. The majority of PIP4Kα was cytosolic with a small amount that was nuclear. Although RNAi suppressed the expression of PIP4Kβ to 15% of the control level, the total amount of PIP4Kα present in the nucleus was not reduced significantly. This suggests that translocation of PIP4Kα into the nucleus may not be solely dependent on its interaction with PIP4Kβ (Figure 6A). As the antibodies against PIP4Kα cannot be used to immunolocalise the endogenous protein, Myc-PIP4Kα was expressed alone or together with HA-PIP4Kβ and their subcellular distribution was determined using confocal microscopy. Overexpressed Myc-PIP4Kα was found predominantly in the cytosol with some staining in the nucleus (Figure 6B). PIP4Kβ on the other hand was present both in the cytoplasm and in nuclear speckles (Figure 6C). When the two enzymes were co-expressed the localisation of PIP4Kβ remained unchanged but PIP4Kα could be clearly observed in nuclear speckles that co-localised with PIP4Kβ (see merge in Figure 6D). These data indicate that while PIP4Kβ may not control the overall nuclear import of PIPKα, it may modulate the sub-nuclear localisation of PIP4Kα.

Although it is difficult to determine the absolute amounts of PIP4Kα and β using antibodies and western blotting, we investigated the amount of PIP4Kα associated with PIP4Kβ in each subcellular fraction. Western blotting of PIP4Kβ immunoprecipitates from the membrane fraction, revealed that the molecular weights of PIP4Kα and β were smaller when compared to their cytosolic counterparts (Figure 6E). These bands are the correct proteins as they are not present in the RNAi PIP4Kβ knockdown lines. The decrease in molecular weight may be a consequence of post-translational modification or alternatively, of proteolytic processing. Strikingly, the ratio of PIP4Kα to PIP4Kβ in the PIP4Kβ immunoprecipitate from nuclear extracts (1.55) was 6 fold higher when compared to the immunoprecipitate from the cytosol (0.21) (Figure 6E). This suggests that that there is a larger percentage of PIP4Kα/PIP4Kβ complex in the nucleus compared to the cytosol. The result is not just a reflection of the total levels of PIP4Kα in the different sub-cellular fractions as the majority (80%) of PIP4Kα is cytosolic (Figure 6A). How the PIP4Kα/ PIP4Kβ complex becomes enriched in the nuclear fraction is not clear. The nucleus may preferentially sequester the PIP4Kα/ PIP4Kβ complex compared to the PIP4Kβ homodimers or the nuclear environment might favour exchange of subunits to generate the hetero-complex.

PIP4Kα affects the ubiquitination of PIP4Kβ by the SPOP/CUL3 complex.

As PIP4Kα can interact with PIP4Kβ, PIP4Kα should play a role in functions that are primarily associated with PIP4Kβ. The nuclear SPOP/CUL3 ubiquitination complex (CUL3 , SPOP and RBX1 (ring-box 1)) can interact with and ubiquitinate PIP4Kβ. Furthermore, the ubiquitination activity of the complex appears to be stimulated by an increase in the level of PtdIns5*P* [24]. How does overexpression of wild type PIP4Kβ, which should decrease the level of PtdIns5*P*, increase its own ubiquitination? We considered that overexpression of PIP4Kβ will increase the level of the PIP4Kβ homodimer, which will have much less PIP4K activity than the PIP4Kα /PIP4Kβ complex, and therefore could potentially act as a dominant negative kinase when recruited to the SPOP/CUL3 complex . This could increase the local level of PtdIns5*P* and therefore increase SPOP/CUL3 mediated ubiquitination of PIP4Kβ. If so, then overexpression of PIP4Kα should rebalance the ratio of the PIP4Kα/PIP4Kβ complex and therefore reduce PIP4Kβ ubiquitination. Furthermore, overexpression of a kinase inactive PIP4Kα would not be expected to suppress PIP4Kβ ubiquitination.

As shown previously [24], ubiquitination of Myc-PIP4Kβ was only observed when it was co-expressed with all three CUL complex proteins (Figure 7A, compare lane 1 with 2 and 7 with 8) and ubiquitination was enhanced when the kinase inactive PIP4Kβ was expressed (Figure 7A, compare lane 2 with 8). Strikingly, co-expression of the wild type PIP4Kα enzyme suppressed ubiquitination of PIP4Kβ (Figure 7A, compare lane 2 with 4 and 8 with 10), however, co-expression of the kinase inactive PIP4Kα (EE-PIP4KαKD) did not (compare lane 2 with 6 and 8 with 12). To test if nuclear PIP4Kα is required to suppress PIP4Kβ ubiquitination, PIP4Kα was targeted to the plasma membrane by a myristoylation sequence and PIP4Kβ ubiquitination was assessed. When co-expressed with PIP4Kβ, Myr-PIP4Kα was not present in the nucleus, localised predominantly on the membrane and did not influence the nuclear localisation of PIP4Kβ (supplementary figure 3). Myr-PIP4Kα is active and *in vivo* can attenuate IpgD induced PtdIns5*P* generation to the same extent as the wild type

PIP4Kα (data not shown). Overexpression of the Myr-PIP4Kα however, did not suppress the ubiquination of the PIP4Kβ (Figure 7B), suggesting that the interaction with PIP4Kβ and targeting of PIP4Kα to the nucleus is required to suppress SPOP/CUL3 mediated PIP4Kβ ubiquitination.

Discussion.

PIP4Kβ exists as a dimer through the interaction between two anti-parallel β-sheets at the N-terminus of the protein [28;30]. When expressed in cells, we also found that PIP4Kβ forms dimers as assessed by sucrose density centrifugation studies. Under these conditions, no monomers were detected. The dimer appeared to be extremely stable as extraction with RIPA buffer containing 0.2% SDS before cross-linking did not prevent dimer formation. The dimeric surface creates a large flat positively charged surface able to interact electrostatically with the membrane [30]. The interaction of PIP4Kβ with the membrane occurs in order to present the enzyme to its substrate PtdIns5*P*, which is then phosphorylated to generate PtdIns(4,5)P_2. However, our studies show that when compared to the PIP4Kα isoform, the PIP4Kβ dimer is 2000 fold less active *in vitro*. This led us to question whether PIP4Kβ is less active *in vivo* than PIP4Kα. Overexpression of IpgD, a bacterial PtdIns(4,5)P_2 4-phosphatase, induced PtdIns5*P* generation which could be partially attenuated by the expression of PIP4Kα, but not by an equivalent level of expression of PIP4Kβ, showing that PIP4Kβ activity is also much lower *in vivo* than PIP4Kα. The inability of PIP4Kβ to decrease IpgD induced PtdIns5*P* levels is not due to its nuclear localisation as we show that PIP4Kβ is present in the cytosol, membrane and in the nucleus.

If the role of both PIP4Kβ and PIP4Kα is to regulate the level of PtdIns5*P*, then the much reduced PIP4K activity of PIP4Kβ is surprising. However, the unexpected discovery that PIP4Kβ interacts with and targets PIP4Kα provides an explanation as to how the low activity PIP4Kβ isoform can regulate PtdIns5*P* levels. They also suggest that the level of nuclear PtdIns5*P* may depend on nuclear PIP4Kα. Whilst we show that PIP4Kα and β can interact with each other, the nature of the interaction is not clear. It is possible that it exists as a heterodimer, or that a PIP4Kα monomer may interact with the PIP4Kβ dimer in a trimeric complex. Indeed, PIP4K purified from erythrocytes showed a native molecular weight of 150000 suggesting the presence of a trimer [31]. Quantitative proteomic studies of PIP4Kα and PIP4Kβ in chicken DT40 cells suggest that the complex of α and β is a dimer. Furthermore, the amino-acid sequence of the β-sheet that forms the dimer interface in PIP4Kβ is identical in PIP4Kα and *in silico* modelling studies confirm the suggestion that PIP4Kα and β could form hetero-dimers [32].

The much lower PIP4K activity of PIP4Kβ compared to PIP4Kα begs the question as to whether there is a role for active PIP4Kβ in the complex. We show that the PIP4K activity is higher when active PIP4Kβ, compared to the inactive PIP4Kβ, is complexed with endogenous PIP4Kα. These data suggest either that PIP4Kα can dramatically stimulate the activity of PIP4Kβ or that PIP4Kβ kinase activity is required to activate PIP4Kα in the complex. The conformation of the active

PIP4Kβ may also be different to the inactive kinase , which may be important for the regulation of the activity of the PIP4Kα subunit. In the absence of specific inhibitors against each isoform and crystal structures of the various complexes it is difficult to conclude the exact role of the active PIP4Kβ subunit in the complex.

It is also pertinent to question whether the formation of the PIP4Kα/β complex is regulated. If the affinities of interaction between PIP4Kβ homodimers and the hetero-complex are similarly equal then the formation of the hetero-complex may just be controlled by the ratio of the levels of expression of PIP4Kα to PIP4Kβ. In this case changes in the ratio of expression of PIP4Kα to PIP4Kβ will modulate the amount of PIP4Kα/PIP4Kβ complex, and therefore the amount of PIP4K activity, targeted by PIP4Kβ. Physiologically, the ratio of the levels of PIP4Kα and PIP4Kβ differ dramatically between tissue types. Perhaps more importantly, the gene encoding PIP4Kβ is located in the ERBB2 amplicon that is often amplified in human breast tumours, which can lead to increased expression of PIP4Kβ [33]. The increased expression of PIP4Kβ could: Increase the concentration of the homodimer, which may have a specific function within the cell, independent of PIP4Kα; Increase targeting of PIP4Kα to decrease PtdIns5*P* levels; Increase the homodimer concentration, which may act in a dominant negative manner and thereby lead to an increase in the level of PtdIns5*P*. Clearly, what the outcome is will very much depend on the absolute ratio of PIP4Kα to PIP4Kβ. Being able to control the expression of PIP4Kβ together with measurement of the PtdIns5*P* level in both the cell and in the nucleus, should clarify some of these issues. Quantitative mass spectrometric evidence for random dimerisation of PIP4Kα and β in chicken DT40 cells are presented in another study [32].

Alternatively or additionally, the hetero-complex formation may be regulated. PIP4Kβ is extensively post-translationally modified (our unpublished data) and these modifications may be able to regulate complex formation. We previously showed that p38 MAP kinase phosphorylates PIP4Kβ at serine 326 and induces a decrease in its PIP4K activity [15]. As PIP4Kα accounts for the majority of PIP4K activity in a PIP4Kβ immunoprecipitate, we considered that the decrease in activity might be due to phosphorylation dependent inhibition of the interaction between PIP4Kα and β. We assessed this and found that UV stimulation, okadaic acid, etoposide, doxorubicin or H_2O_2 treatment did not change the interaction between PIP4Kα and PIP4Kβ (supplementary figure 4), although they did induce serine 326 phosphorylation of PIP4Kβ (data not shown). Phosphorylation of serine 326 on PIP4Kβ may lead to a conformational change that inhibits the activity of the associated PIP4Kα.

Interestingly, in HEK293 cells and in MEL cells (data not shown) the PIP4Kα/β complex appears to be more prevalent in nuclear extracts than in the cytosolic fraction. This does not reflect the total level of PIP4Kα in the two fractions as the majority of PIP4Kα is cytosolic. Notwithstanding that during the nuclear isolation procedure there may be a preferential loss of the PIP4Kβ dimer or of the PIP4Kα enzyme, this may suggest that hetero-complex formation is regulated in the nucleus. We do not believe that there is significant redistribution of the enzymes on sub-cellular fractionation as immunofluorescence analysis of overexpressed PIP4Kα or β show a similar subcellular distribution to subcellular fractionation. Why then is the

PIP4Kα/β complex more prevalent in the nucleus? If the PIP4Kα isoform can only enter the nucleus as a consequence of its interaction with PIP4Kβ, we would expect that the nuclear PIP4Kα/PIP4Kβ ratio would reflect the cytosolic PIP4Kα/PIP4Kβ ratio. The PIP4Kα/PIP4Kβ complex, however, may be preferentially imported into the nucleus or preferentially sequestered in the nucleus compared to the PIP4Kβ homo-dimer. Alternatively, if PIP4Kα can be imported into the nucleus independently of PIP4Kβ then the nuclear environment may favour rapid exchange of subunits to generate the PIP4Kα/PIP4Kβ complex. This may be a direct consequence of sub-cellular specific post-translational modification of PIP4Kβ. PIP4Kα may be imported into the nucleus independently of PIP4Kβ as, compared to control cells, we were unable to detect significant differences in the total amount of PIP4Kα present in the nucleus after PIP4Kβ expression was suppressed by RNAi.

It is clear, however, that control of the nuclear localisation of both PIP4Kβ and α is complex. Previous studies on the overexpression of PIP4Kβ in HeLa cells [16] and on the localisation of flag-tagged endogenous PIP4Kβ in Chicken DT40 cells [34] suggested that the majority of PIP4Kβ was nuclear. However, in most cells that we have studied, overexpressed PIP4Kβ localises to the nucleus, the cytosol and the plasma membrane as observed by others [24] and in this study in HeLa cells. However, in MCF7 cells the majority of PIP4Kβ appears nuclear while in T47D, another breast cancer cell line, PIP4Kβ is mainly cytosolic (data not shown). The reason for these differences is not clear but may be a consequence of differential expression of import factors or post-translational modification of PIP4Kβ. In the case of PIP4Kα in HT1080 cells, overexpressed PIP4Kα is predominantly cytosolic. Co-overexpression of PIP4Kα and PIP4Kβ leads to a clear increase in total PIP4Kα targeted to the nucleus (supplementary Figure 5) suggesting that in some cells, overexpressed PIP4Kβ will target more PIP4Kα into the nucleus. Our data also show that PIP4Kβ can target PIP4Kα to nuclear speckles and that PIP4Kβ mediated targeting of PIP4Kα is functional and can regulate the ubiquitination activity of the SPOP/CUL3 complex.

The ability of inactive mutant proteins to localise or modulate active counterparts has been reported in numerous signalling cascades and has been well characterised in the myotubularin family. Myotubularins are a family of lipid phosphatases some of which are inactive, such as MTMR13, due to a mutation in a critical active site cysteine residue [35]. MTMR13 interacts with and activates MTMR2 [36] and mutation in either MTMR2 or the inactive MTMR13 can induce Charcot Marie tooth syndrome 4B [37]. These data exemplify the importance of how the interaction between the active PIP4Kα and less active PIP4Kβ may impinge on phosphoinositide regulation in physiological and pathological conditions.

Acknowledgments.

We would like to note that while this work was in progress we became aware that another group independently discovered the association between PIP4Kα and PIP4Kβ [32]. We would like to acknowledge previous colleagues at the NKI and the Dutch cancer society for funding. IpgD was from B. Payrastre, CUL3, RBX and SPOP were from M.Van Lohuizen and pSuper and pRetroSuper plasmids from R. Agami. We thank all members of the inositide laboratory for helpful discussions during the preparation of this manuscript and to members of Leukaemia biology. We would also like to acknowledge the efforts of the Duncan Smith and the mass spectrometry unit and all core facilities at the PICR.

Figure legends

Figure 1

A. Nuclear extracts from HEK293 cells expressing HA-PIP4Kβ were separated by sucrose density centrifugation and each fraction was separated by SDS-PAGE and the gel was stained with silver. The western blot below shows the presence of the BRG1 complex (>500000 kDa) in fractions 12-15. 2 ul of every fraction from the sucrose density centrifugation of cytosolic or nuclear fraction was spotted onto nitrocellulose and probed with the anti-HA antibody and relevant fractions containing HA immunoreactivity were analysed by western blotting. B. MEL cell nuclei were treated with increasing concentrations of the irreversible cross-linking agent DSS. Nuclear extracts were then immunoprecipitated with either a pre-immune serum or a PIP4Kβ specific serum (p5 or p6) and western blotted with an anti-PIP4K rat monoclonal antibody (Antibody 3). Increasing concentrations of DSS induced the formation of the cross linked dimer (arrow). C. Nuclei were treated as shown, extracted and immunoprecipitated with the indicated antibodies. The western blot was probed with a specific rat monoclonal antibody against PIP4K (Antibody 3). The data shown are representative of at least two different experiments.

Figure2.

A. HA-PIP4Kβ was purified from HEK293 cells expressing HA-PIP4Kβ using HA-immunoaffinity chromatography. Eluted proteins were separated by SDS-PAGE and the coomassie stained gel was cut into 60 slices and each slice was analysed by mass spectrometry. The figure shows the peptides which uniquely defined the presence of PIP4Kα (top) or PIP4Kβ (bottom), in fractions 33 and 34. B. The lysate from HEK293 cells expressing Myc-PIP4Kβ (lane 1) was used for affinity purification with either GST (lane 2), GST-PIP4Kα (lane 3), GST-PIP4Kβ (lane 4) or GST-PIP4Kγ (lane5). Bound proteins were analysed by western blotting using an anti-Myc antibody. Lane 1 shows 10% of the lysate input used for each affinity purification. C. EE-PIP4Kα and HA-PIP4Kβ were expressed in HEK293 cells, as indicated (below) and immunoprecipitated and western blotted with the indicated antibodies. The experiment is representative of three separate experiments. D. HA-PIP4Kβ purified from HEK293 cells was combined with purified bacterially expressed PIP4Kα, after removal of the GST-tag by thrombin cleavage, incubated at room temperature for one hour and then immunoprecipitated using the anti-HA antibody. Immunoprecipitates were analysed by western blot and were probed first for PIP4Kα (top panel) after which the blot was stripped and reprobed with an anti-HA antibody (lower panel). 10% of the total protein input was also western blotted. The arrow denotes PIP4Kα co-immunoprecipitated in the HA-immunoprecipitate.

Figure 3.

A. Lysates, from HEK293 stably expressing the indicated pRetroSuper construct, were probed using the antibodies shown. RNAi to PIP4Kα suppressed its expression to 54% of the control value while the RNAi to PIP4Kβ suppressed its expression to 15% of the control value. B. Lysates from HEK293 stably expressing the indicated RNAi construct were

immunoprecipitated with the antibodies shown and the western blot was probed with an anti-PIP4Kα antibody. The blot was stripped and reprobed with an anti-PIP4Kβ antibody. C. Lysates from HEK293 stably expressing the indicated RNAi construct were immunoprecipitated as indicated and the western blot was probed for the presence of PIP4Kβ. The blot was stripped and reprobed for PIP4Kα. The data are representative of three separate experiments.

Figure 4

A. Purified GST-PIP4Kα and β were quantitated by SDS-PAGE and coomassie blue staining (top panel). Matched quantities of protein were then assayed for PIP4K activity (autoradiograph middle panel and quantitation in the graph and box). B. Myc-PIP4Kα and β were purified from HEK293 cells and quantitated by western blots probed with the anti-Myc antibody (top panel). Matched inputs were assayed for PIP4K activity (autoradiograph middle panel and quantitation in the graph and box). C PIP4Kα (left) or PIP4Kβ (right) activity was assayed using liposomes containing PtdSer (50nmol) and increasing amounts of PtdIns5*P*. The data is represented graphically and the kinetic parameters (Km and Vmax) were determined and are shown in the table. Note that for the graph the phosphoimaging exposure time for the PIP4Kα was 5 minutes while the exposure time for PIP4Kβ was 90 minutes D. PtdIns5*P* was measured in HEK293 cells transfected as indicated. Expression of the various constructs are shown in the top panels while PtdIns5*P* levels are shown in the graph.

Figure 5

HEK293 cells were transfected with the constructs shown and the lysates were divided and immunoprecipitated using an antibody against the EE (left panel) or HA-tag (right panel). Immunoprecipitates were split and PIP4K activity was assessed (graph) and the rest was analysed by western blotting using the indicated antibodies (top blot). The blot was stripped and then reprobed with the indicated antibodies (bottom blot). It appears that PIP4KαKD interacts less well with PIP4Kβ, however this is a consequence of its lower expression (see left blot EE-IP WB PIP4Kα). The ratio of PIP4Kα/PIP4KαKD in the input is 3.95 and is similar in the PIP4Kβ immunoprecipitate (4.4). B. Membrane, cytosol and nuclear fractions were isolated from HEK293 cells expressing either pRetroSuper or RNAi PIP4Kα and lysates from these fractions were immunoprecipitated with p19 (anti-PIP4Kα) and PIP4K activity was measured. C. Cytosol/membrane and nuclear fractions from the above cell lines were immunoprecipitated with p6 (anti-PIP4Kβ). The immunoprecipitates were divided and assessed for PIP4K activity (graph), and analysed by western blotting with antibodies to endogenous PIP4Kα (upper right panel). The blot was stripped and reprobed for PIP4Kβ (lower right panel). D. HEK293 cells were transfected with the indicated siRNA oligos and lysates were immunoprecipitated as indicated, split and assayed for PIP4K activity (numbers on the graph indicate % of control) and western blotted with the indicated antibodies. E. Wild type or kinase inactive (D278A) Myc-PIP4Kβ was expressed in control cells (pRetroSuper) or cells suppressed for the expression of PIP4Kα (RNAi PIP4Kalpha). Cell lysates were immunoprecipitated

with the anti-Myc antibody and assayed for PIP4K activity (graph) and western blotted for the co-IP of endogenous PIP4Kα (Arrow upper panel). The blot was then stripped and reprobed for Myc-PIP4Kβ (lower panel). The data are representative of at least two separate experiments.

Figure 6.

A. Lysates from cytosol and nuclear fractions, isolated from HEK293 expressing the indicated RNAi constructs, were immunoprecipitated with an antibody specific for PIP4Kα (p19) and western blotted using the antibody against PIP4Kα. B. HeLa cells were transfected with Myc-PIP4Kα, fixed and stained using the anti-Myc antibody. C. Cells were transfected with HA-PIP4Kβ and stained using the anti-HA antibody. D. Cells were co-transfected with Myc-PIP4Kα and HA-PIP4Kβ, fixed and stained with rabbit anti-Myc antibody (left micrograph) and mouse anti-HA (middle micrograph) and the merge is shown on the right. E. Lysates from HEK293 cells stably expressing the RNAi constructs indicated, were immunoprecipitated with p6 (anti-PIP4Kβ) and western blotted for PIP4Kα (top panel). The blot was stripped and reprobed with p6 (anti-PIP4Kβ). The data show that the ratio of PIP4Kα to PIP4Kβ in a PIP4Kβ immunoprecipitate is higher in the nuclear extracts (1.55) compared to the cytosol (0.21). The arrows denote the different molecular weights of PIP4Kα in the membrane, cytosol and nuclear fraction. The data are representative of at least two separate experiments

Figure 7.

A. HEK293 cells were transfected as indicated and His-tagged proteins were affinity purified using nickel sepharose and analysed by western blotting with an anti-Myc antibody to visualise Myc-PIP4Kβ and its ubiquitinated products. The arrow denotes where non-ubiquitinated Myc-PIP4Kβ would migrate. Total cell lysates were also separated by SDS-PAGE and probed as shown. B. His-tagged proteins were purified from lysates of cells expressing the indicated constructs and analysed by western blotting using a Myc-antibody. Total cell lysates were also western blotted with the indicated antibodies. Note all cells received the three CUL complex proteins (CUL, RBX and SPOP). The data are representative of three separate experiments.

Reference List

1 Irvine, R. F. (2005) Inositide evolution - towards turtle domination? J.Physiol, **566**, 295-300.

2 McCrea, H. J. and DeCamilli P. (2009) Mutations in phosphoinositide metabolizing enzymes and human disease. Physiology.(Bethesda.), **24**, 8-16.

3 van den Bout, I. and Divecha, N. (2009) PIP5K-driven PtdIns(4,5)P2 synthesis: regulation and cellular functions. J.Cell Sci., **122**, 3837-3850.

4 Loijens, J. C., Boronenkov, I. V., Parker, G. J. and Anderson, R. A. (1996) The phosphatidylinositol 4-phosphate 5-kinase family. Adv.Enzyme Regul., **36**:115-40,.

5 Rameh, L. E., Tolias, K. F., Duckworth, B. C. and Cantley, L. C. (1997) A new pathway for synthesis of phosphatidylinositol-4,5-bisphosphate. Nature, **390**, 192-196.

6 Divecha, N., Truong, O., Hsuan, J. J., Hinchliffe, K. A. and Irvine, R. F. (1995) The cloning and sequence of the C isoform of PtdIns4P 5-kinase. Biochem.J., **309**, 715-719.

7 Boronenkov, I. V. and Anderson, R. A. (1995) The sequence of phosphatidylinositol-4-phosphate 5-kinase defines a novel family of lipid kinases. J.Biol.Chem., **270**, 2881-2884.

8 Castellino, A. M., Parker, G. J., Boronenkov, I. V., Anderson, R. A. and Chao, M. V. (1997) A novel interaction between the juxtamembrane region of the p55 tumor necrosis factor receptor and phosphatidylinositol-4- phosphate 5-kinase. J.Biol.Chem., **272**, 5861-5870.

9 Itoh, T., Ijuin, T. and Takenawa, T. (1998) A novel phosphatidylinositol-5-phosphate 4-kinase (phosphatidylinositol- phosphate kinase IIgamma) is phosphorylated in the endoplasmic reticulum in response to mitogenic signals. J.Biol.Chem., **273**, 20292-20299.

10 Zhang, X., Loijens, J. C., Boronenkov, I. V., Parker, G. J., Norris, F. A., Chen, J., Thum, O., Prestwich, G. D., Majerus, P. W. and Anderson, R. A. (1997) Phosphatidylinositol-4-phosphate 5-kinase isozymes catalyze the synthesis of 3-phosphate-containing phosphatidylinositol signaling molecules. J.Biol.Chem., **272**, 17756-17761.

11 Clarke, J. H., Emson, P. C. and Irvine, R. F. (2008) Localization of phosphatidylinositol phosphate kinase IIgamma in kidney to a membrane trafficking compartment within specialized cells of the nephron. Am.J.Physiol Renal Physiol, **295**, F1422-F1430.

12 Schulze, H., Korpal, M., Hurov, J., Kim, S. W., Zhang, J., Cantley, L. C., Graf, T. and Shivdasani, R. A. (2006) Characterization of the megakaryocyte demarcation membrane system and its role in thrombopoiesis. Blood, **107**, 3868-3875.

13 Rozenvayn, N. and Flaumenhaft, R. (2001) Phosphatidylinositol 4,5-bisphosphate mediates Ca2+-induced platelet alpha-granule secretion: evidence for type II phosphatidylinositol 5-phosphate 4-kinase function. J.Biol.Chem., **276**, 22410-22419.

14 Rozenvayn, N. and Flaumenhaft, R. (2003) Protein kinase C mediates translocation of type II phosphatidylinositol 5-phosphate 4-kinase required for platelet alpha-granule secretion. J.Biol.Chem., **278**, 8126-8134.

15 Jones, D. R., Bultsma, Y., Keune, W. J., Halstead, J. R., Elouarrat, D., Mohammed, S., Heck, A. J., D'Santos, C. S. and Divecha, N. (2006) Nuclear PtdIns5P as a transducer of stress signaling: an in vivo role for PIP4Kbeta. Mol.Cell, **23**, 685-695.

16 Ciruela, A., Hinchliffe, K. A., Divecha, N. and Irvine, R. F. (2000) Nuclear targeting of the beta isoform of type II phosphatidylinositol phosphate kinase (phosphatidylinositol 5-phosphate 4-kinase) by its alpha-helix 7. Biochem.J., **346** 587-591.

17 Castellino, A. M. and Chao, M. V. (1999) Differential association of phosphatidylinositol-5-phosphate 4- kinase with the EGF/ErbB family of receptors. Cell Signal., **11**, 171-177.

18 Lamia, K. A., Peroni, O. D., Kim, Y. B., Rameh, L. E., Kahn, B. B. and Cantley, L. C. (2004) Increased insulin sensitivity and reduced adiposity in phosphatidylinositol 5-phosphate 4-kinase beta-/- mice. Mol.Cell Biol., **24**, 5080-5087.

19 Carricaburu, V., Lamia, K. A., Lo, E., Favereaux, L., Payrastre, B., Cantley, L. C. and Rameh, L. E. (2003) The phosphatidylinositol (PI)-5-phosphate 4-kinase type II enzyme controls insulin signaling by regulating PI-3,4,5-trisphosphate degradation. Proc.Natl.Acad.Sci.U.S.A, **19;100**, 9867-9872.

20 Ramel, D., Lagarrigue, F., Dupuis-Coronas, S., Chicanne, G., Leslie, N., Gaits-Iacovoni, F., Payrastre, B. and Tronchere, H. (2009) PtdIns5P protects Akt from dephosphorylation through PP2A inhibition. Biochem.Biophys.Res.Commun., **387**, 127-131.

21 Gozani, O., Karuman, P., Jones, D. R., Ivanov, D., Cha, J., Lugovskoy, A. A., Baird, C. L., Zhu, H., Field, S. J., Lessnick, S. L., Villasenor, J., Mehrotra, B., Chen, J., Rao, V. R., Brugge, J. S., Ferguson, C. G., Payrastre, B., Myszka, D. G., Cantley, L. C., Wagner, G., Divecha, N., Prestwich, G. D. and Yuan, J. (2003) The PHD finger of the chromatin-associated protein ING2 functions as a nuclear phosphoinositide receptor. Cell, **114**, 99-111.

22 Alvarez-Venegas, R., Sadder, M., Hlavacka, A., Baluska, F., Xia, Y., Lu, G., Firsov, A., Sarath, G., Moriyama, H., Dubrovsky, J. G. and Avramova, Z. (2006) The Arabidopsis homolog of trithorax, ATX1, binds phosphatidylinositol 5-phosphate, and the two regulate a common set of target genes. Proc.Natl Acad.Sci.U.S.A., **103**, 6049-6054.

23 Elkin, S. K., Ivanov, D., Ewalt, M., Ferguson, C. G., Hyberts, S. G., Sun, Z. Y., Prestwich, G. D., Yuan, J., Wagner, G., Oettinger, M. A. and Gozani, O. P. (2005) A PHD finger motif in the C terminus of RAG2 modulates recombination activity. J Biol Chem, **280**, 28701-28710.

24 Bunce, M. W., Boronenkov, I. V. and Anderson, R. A. (2008) Coordinated activation of the nuclear ubiquitin ligase Cul3-SPOP by the generation of phosphatidylinositol 5-phosphate. J.Biol.Chem., **283**, 8678-8686.

25 Brooksbank, C. E., Hutchings, A., Butcher, G. W., Irvine, R. F. and Divecha, N. (1993) Monoclonal antibodies to phosphatidylinositol 4-phosphate 5- kinase: distribution and intracellular localization of the C isoform. Biochem.J., **291**, 77-82.

26 Jones, D. R., Bultsma, Y., Keune, W. J. and Divecha, N. (2009) Methods for the determination of the mass of nuclear PtdIns4P, PtdIns5P, and PtdIns(4,5)P2. Methods Mol.Biol., **462**, 75-88.

27 Clarke, J. H., Letcher, A. J., D'Santos, C. S., Halstead, J. R., Irvine, R. F. and Divecha, N. (2001) Inositol lipids are regulated during cell cycle progression in the nuclei of murine erythroleukaemia cells. Biochem.J., **357**, 905-910.

28 Rao, V. D., Misra, S., Boronenkov, I. V., Anderson, R. A. and Hurley, J. H. (1998) Structure of type IIbeta phosphatidylinositol phosphate kinase: a protein kinase fold flattened for interfacial phosphorylation. Cell, **94**, 829-839.

29 Niebuhr, K., Giuriato, S., Pedron, T., Philpott, D. J., Gaits, F., Sable, J., Sheetz, M. P., Parsot, C., Sansonetti, P. J. and Payrastre, B. (2002) Conversion of PtdIns(4,5)P(2) into PtdIns(5)P by the S.flexneri effector IpgD reorganizes host cell morphology. EMBO J., **21**, 5069-5078.

30 Burden, L. M., Rao, V. D., Murray, D., Ghirlando, R., Doughman, S. D., Anderson, R. A. and Hurley, J. H. (1999) The flattened face of type II beta phosphatidylinositol phosphate kinase binds acidic phospholipid membranes. Biochemistry, **38**, 15141-15149.

31 Ling, L. E., Schulz, J. T. and Cantley, L. C. (1989) Characterization and purification of membrane-associated phosphatidylinositol-4-phosphate kinase from human red blood cells. J.Biol.Chem., **264**, 5080-5088.

32 Wang, Minchuan, Bond, Nicholas, Letcher, A. J., Richardson, Jonathon P, Lilley, Kathryn S, Irvine, Robin F, and Clarke, Jonathon H. Genomic tagging reveals a random association of endogenous PtdIns5P 4-kinases IIa and IIb and a partial nuclear localisation of the IIa isoform. submitted . 2010.

33 Luoh, S. W., Venkatesan, N. and Tripathi, R. (2004) Overexpression of the amplified Pip4k2beta gene from 17q11-12 in breast cancer cells confers proliferation advantage. Oncogene, **19;23**, 1354-1363.

34 Richardson, J. P., Wang, M., Clarke, J. H., Patel, K. J. and Irvine, R. F. (2007) Genomic tagging of endogenous type IIbeta phosphatidylinositol 5-phosphate 4-kinase in DT40 cells reveals a nuclear localisation. Cell Signal., **19**, 1309-1314.

35 Laporte, J., Bedez, F., Bolino, A. and Mandel, J. L. (2003) Myotubularins, a large disease-associated family of cooperating catalytically active and inactive phosphoinositides phosphatases. Hum.Mol.Genet., **12** Spec No 2, R285-R292.

36 Robinson, F. L. and Dixon, J. E. (2005) The phosphoinositide-3-phosphatase MTMR2 associates with MTMR13, a membrane-associated pseudophosphatase also mutated in type 4B Charcot-Marie-Tooth disease. J.Biol.Chem., **280**, 31699-31707.

37 Azzedine, H., Bolino, A., Taieb, T., Birouk, N., Di, D. M., Bouhouche, A., Benamou, S., Mrabet, A., Hammadouche, T., Chkili, T., Gouider, R., Ravazzolo, R., Brice, A., Laporte, J. and LeGuern, E. (2003) Mutations in MTMR13, a new pseudophosphatase homologue of MTMR2 and Sbf1, in two families with an autosomal recessive demyelinating form of Charcot-Marie-Tooth disease associated with early-onset glaucoma. Am.J.Hum.Genet., **72**, 1141-1153.

Biochemical Journal Immediate Publication. Published on 28 Jun 2010 as manuscript BJ20100341

Figure 1

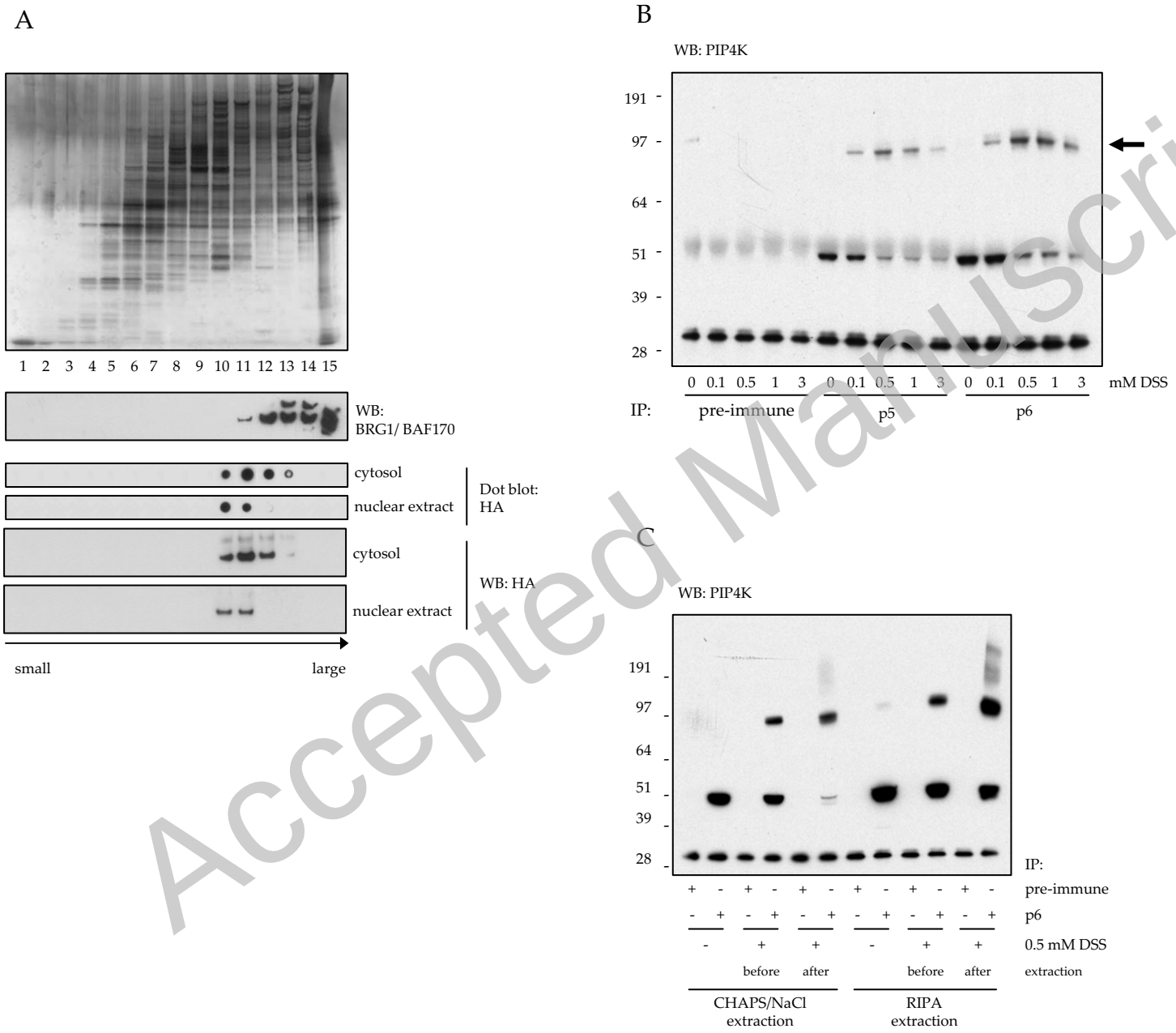

Biochemical Journal Immediate Publication. Published on 28 Jun 2010 as manuscript BJ20100341

Figure 2

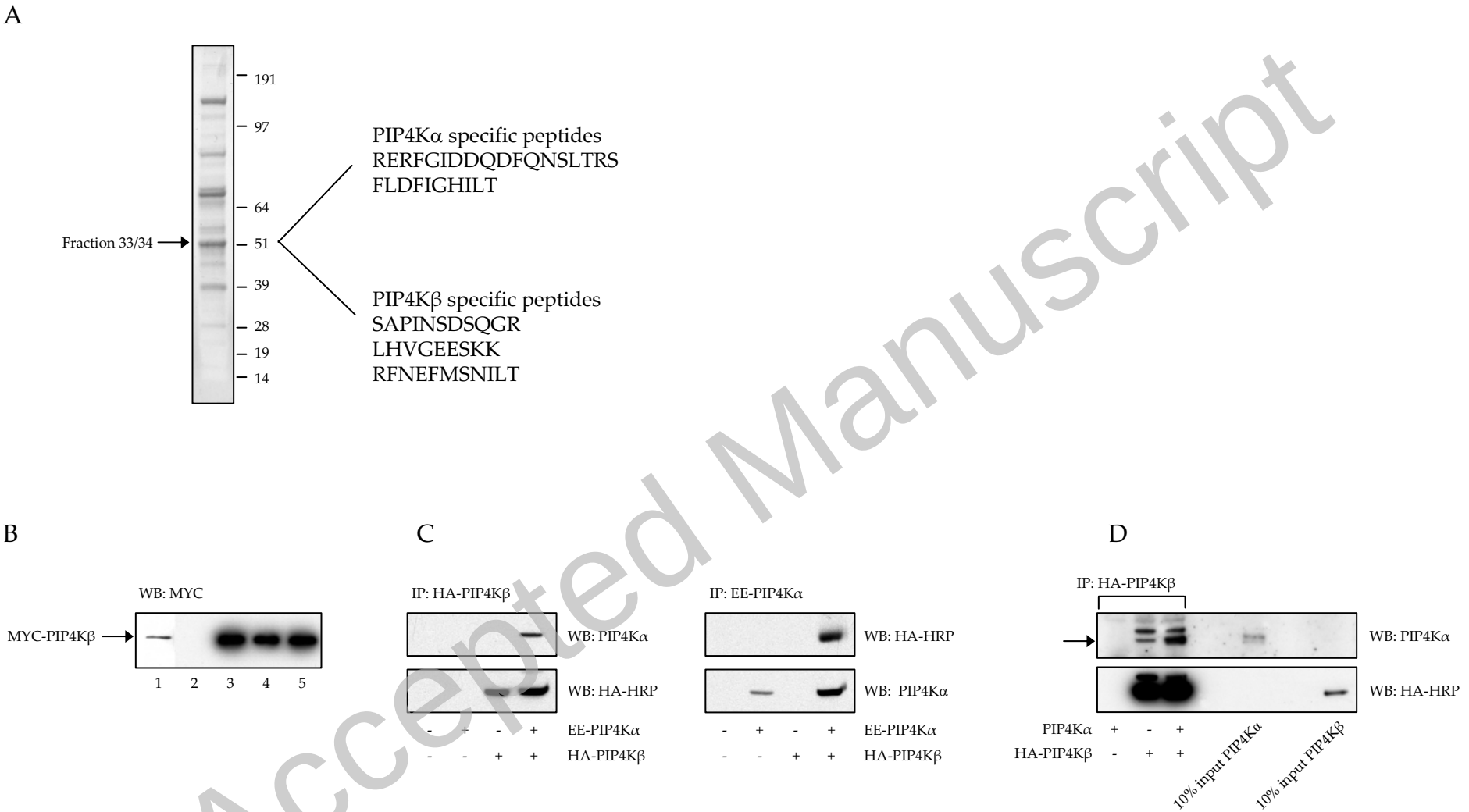

Biochemical Journal Immediate Publication. Published on 28 Jun 2010 as manuscript BJ20100341

Figure 3

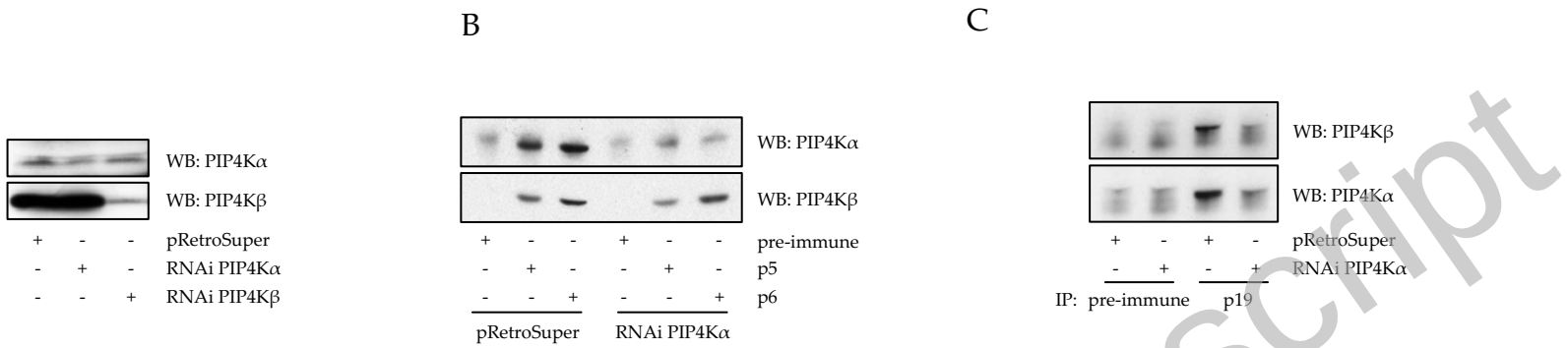

Biochemical Journal Immediate Publication. Published on 28 Jun 2010 as manuscript BJ20100341

Figure 4

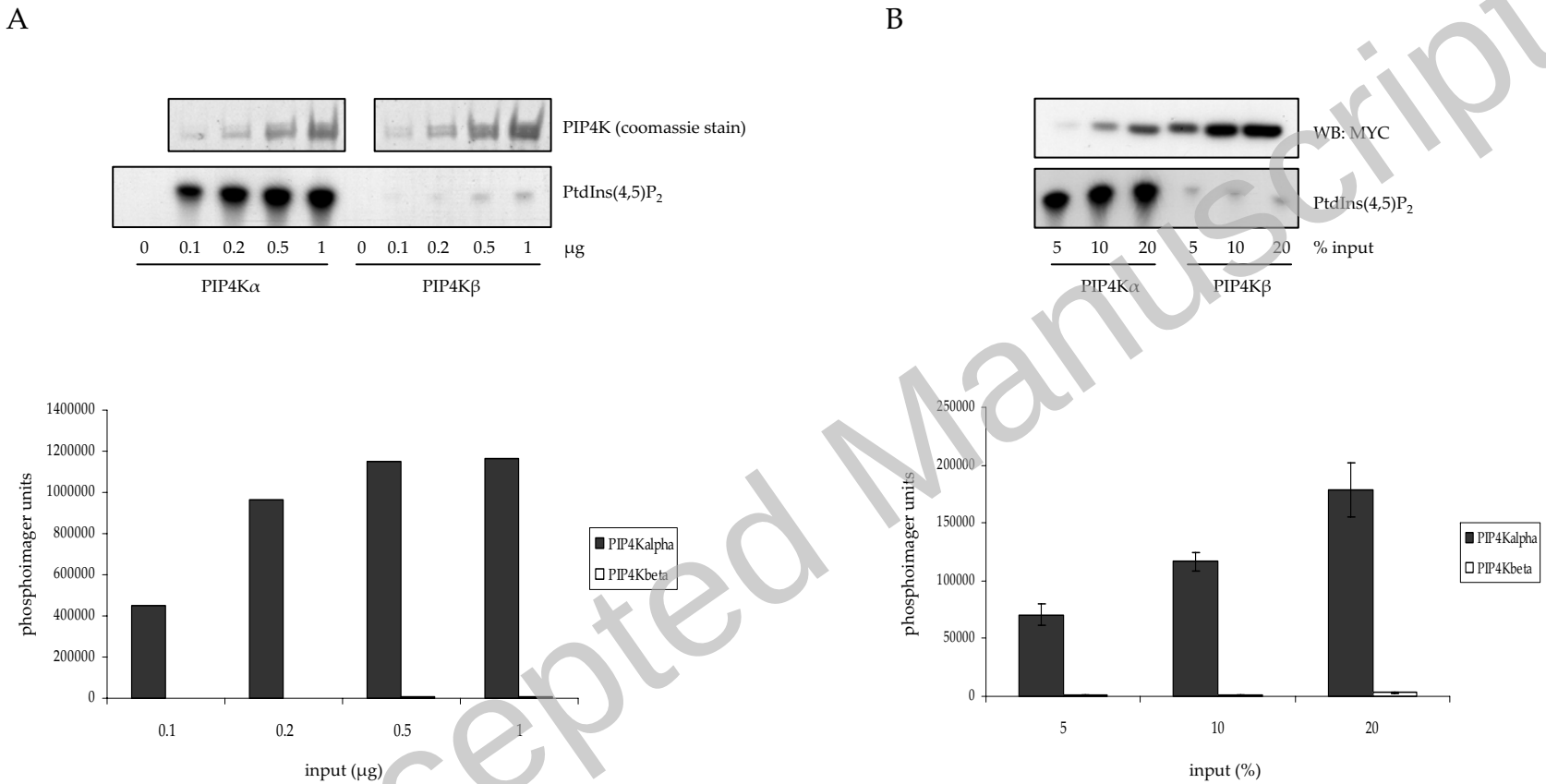

	Specific activity (counts/ µg protein)	fold
GST-PIP4Kα	4662.2 ± 228.9 *10^3	434
GST-PIP4Kβ	10.8 ± 2.4 *10^3	1

	Specific activity (counts/protein)	fold
MYC-PIP4Kα	1139.8 ± 277.8	207
MYC-PIP4Kβ	5.5 ± 3.2	1

Biochemical Journal Immediate Publication. Published on 28 Jun 2010 as manuscript BJ20100341

Figure 4

C

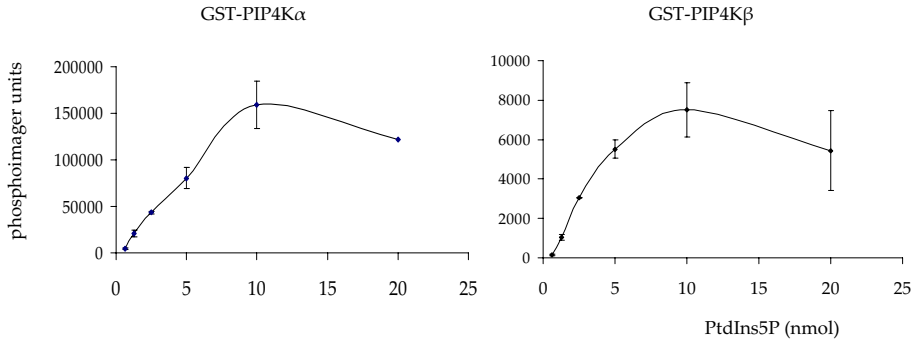

	Vmax (pmol/min/μg)	Km (μM)
GST-PIP4Kα	466.00 ± 30.56	50
GST-PIP4Kβ	0.202 ± 0.014	30

D

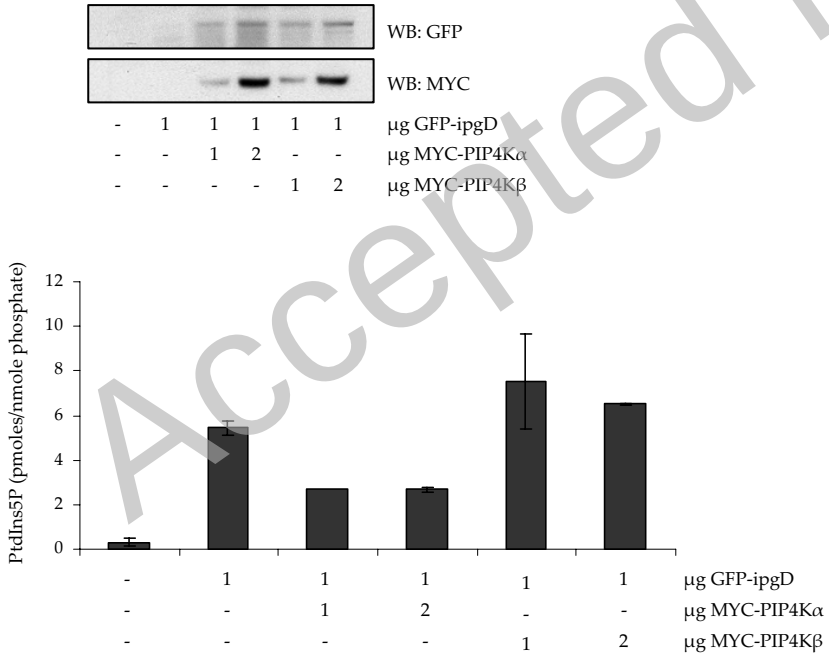

Biochemical Journal Immediate Publication. Published on 28 Jun 2010 as manuscript BJ20100341

Figure 5

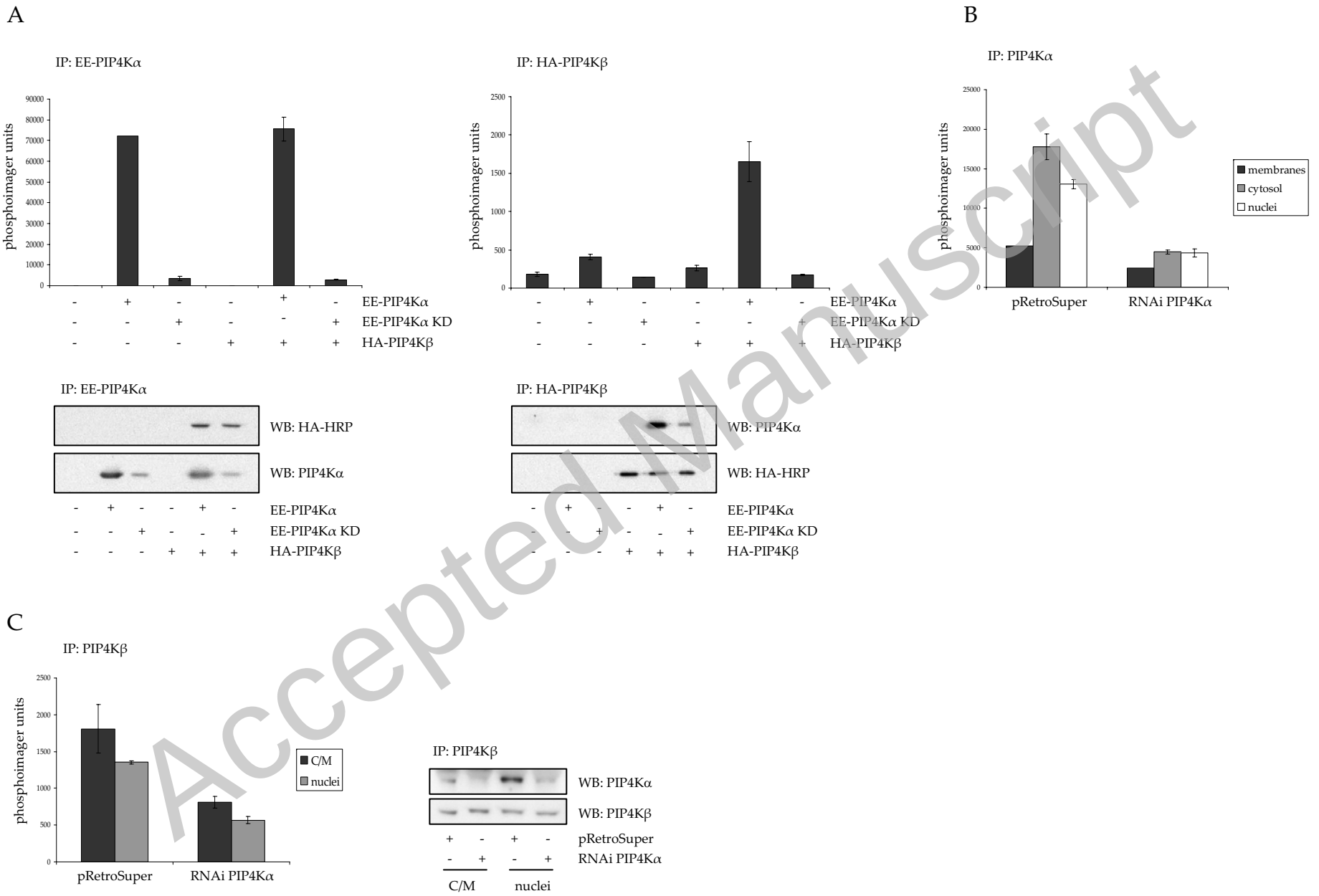

Biochemical Journal Immediate Publication. Published on 28 Jun 2010 as manuscript BJ20100341

Figure 5

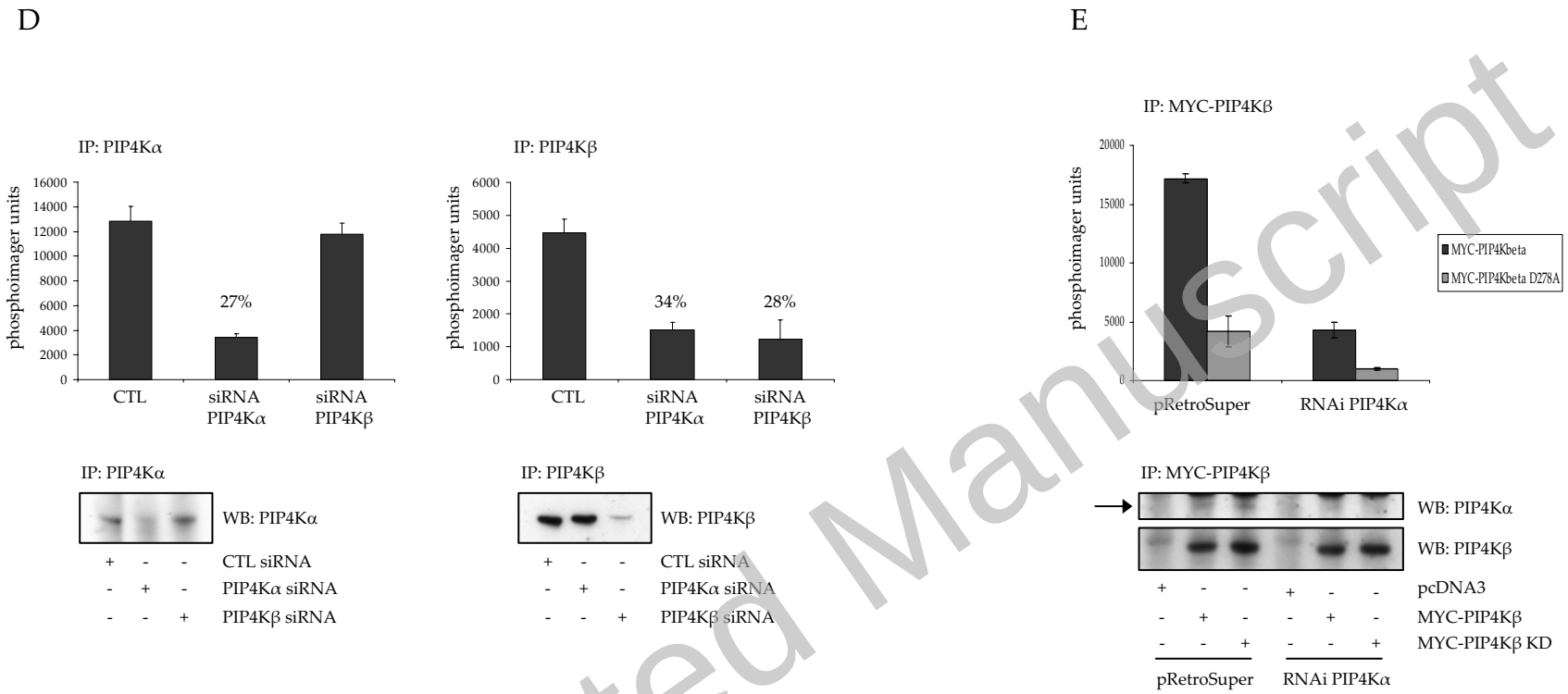

Biochemical Journal Immediate Publication. Published on 28 Jun 2010 as manuscript BJ20100341

Figure 6

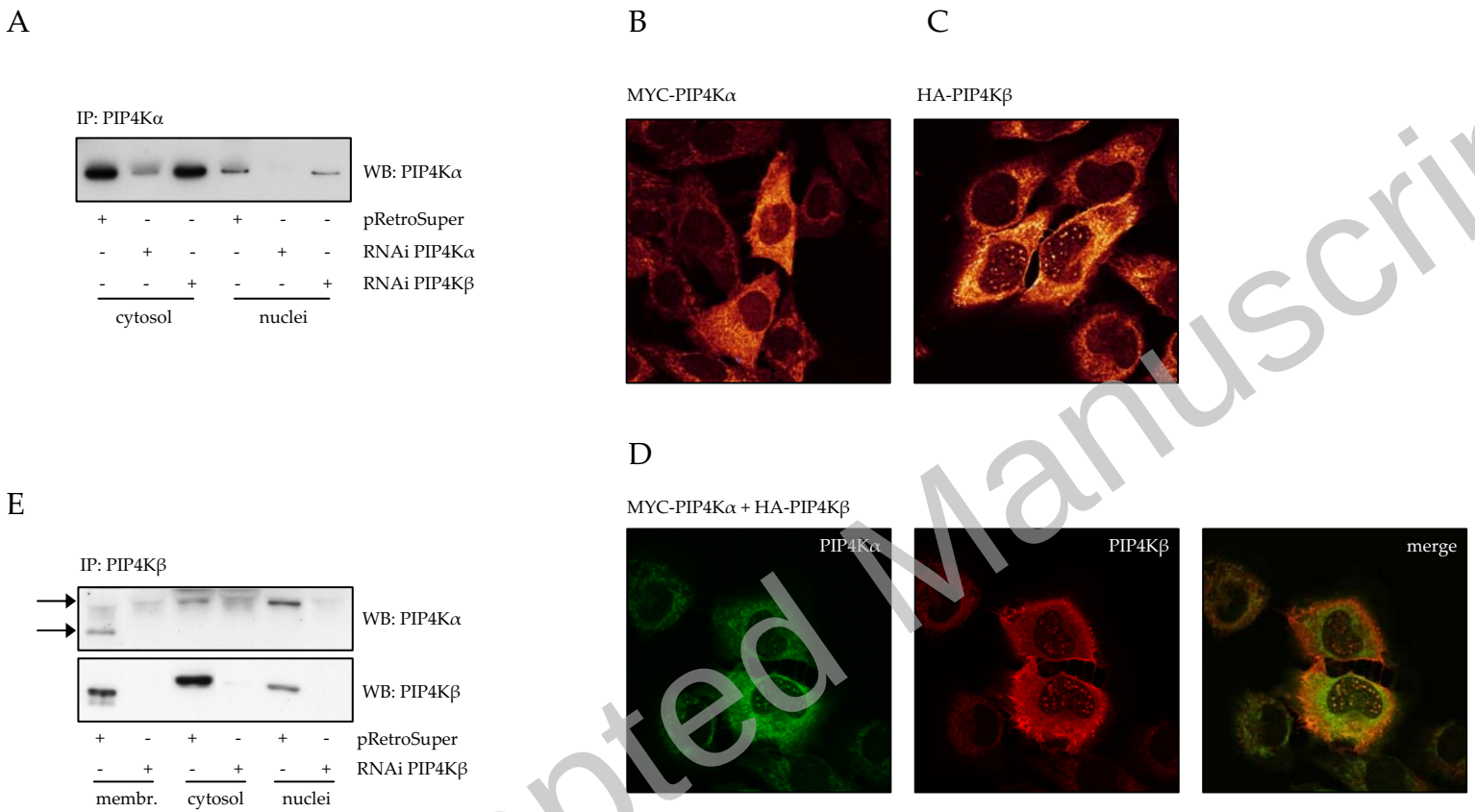

Biochemical Journal Immediate Publication. Published on 28 Jun 2010 as manuscript BJ20100341

Figure 7